arXiv:1110.0485v1 [astro-ph.SR] 3 Oct 2011

The nature and consequences of clumping in hot, massive star winds

Jon O. Sundqvist[1], Stanley P. Owocki[1], and Joachim Puls[2]

[1]*University of Delaware, Bartol Research Institute, Newark, Delaware 19716, USA*

[2]*Universitätssternwarte München, Scheinerstr. 1, 81679 München, Germany*

Abstract.   This review describes the evidence for small-scale structure, 'clumping', in the radiation line-driven winds of hot, massive stars. In particular, we focus on examining to what extent simulations of the strong instability inherent to line-driving can explain the multitude of observational evidence for wind clumping, as well as on how to properly account for extensive structures in density and velocity when interpreting the various wind diagnostics used to derive mass-loss rates.

1.   Introduction

Hot, massive stars possess strong stellar winds driven by line scattering of the star's intense continuum radiation field. The first quantitative description of such line driving was given in the seminal paper by Castor et al. (1975, 'CAK'), assuming a stationary, homogeneous, and spherically symmetric wind. But despite the considerable success of subsequent work assuming such a smooth, steady outflow (e.g., Vink et al. 2000), the theoretical as well as observational evidence for a time-dependent, inhomogeneous wind is irrefutable (Puls et al. 2008; Hamann et al. 2008). This review summarizes the current status concerning small-scale inhomogeneities, 'clumping', in the winds of single hot stars; for an overview of large-scale wind inhomogeneities, induced by for example rapid rotation or a strong magnetic field, see Puls et al. (2008). After first outlining the theoretical basis in terms of a strong instability inherent to line driving, we next concentrate on confronting predictions of corresponding instability models with a subset of the large body of direct and indirect observational evidence for wind clumping. In particular we focus on the consequences of extensive density and velocity structure when interpreting various mass-loss diagnostics.

2.   Theory: the line driven instability

Linear stability analysis showed already early on that the line-driven winds of hot stars should be unstable for velocity perturbations on scales near and below the Sobolev length $L_{Sob} = v_{th}/(dv/dr)$ (MacGregor et al. 1979; Carlberg 1980; Owocki & Rybicki 1984). The operation of this strong, intrinsic 'line-driven instability' (LDI) has since been confirmed by direct numerical modeling of the time-dependent wind (Owocki et al. 1988; Feldmeier 1995; Dessart & Owocki 2005a). Such simulations typically show that the non-linear growth of the LDI leads to high-speed rarefactions that steepen into

strong reverse shocks, whereby most of the wind material is compressed into dense and spatially narrow 'clumps' that are separated by large regions of much lower densities. This characteristic structure is the theoretical basis for our current understanding and interpretation of *wind clumping*.

The left panel of Fig. 1 illustrates this typical structure by plotting density and velocity snapshots of a 1-D LDI simulation computed from an initial steady CAK model following Feldmeier et al. (1997) (see Sundqvist et al. 2011b, for model specific details). The line force is calculated using the 'Smooth Source function' method (SSF, Owocki & Puls 1996), which allows one to follow the non-linear evolution of the strong, intrinsic instability, while also accounting for the stabilizing line drag effect of the scattered, diffuse radiation field (Lucy 1984). The simulation here further introduces base perturbations from Langevin turbulence (see Feldmeier et al. 1997), which induce structure somewhat closer to the wind base as compared to simulations with self-excited structure formation (Runacres & Owocki 2002, 2005). But despite these seed perturbations, the line drag from the SSF force greatly reduces, even eliminates, the instability near the base, thus allowing the lowermost wind to remain smooth and steady (Fig. 1).
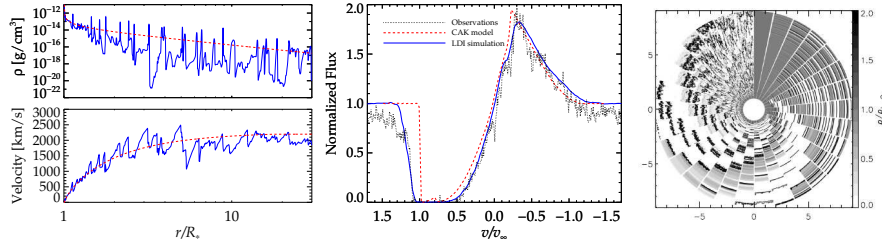

Figure 1.   **Left:** Snapshot of density and velocity structure in a 1-D LDI simulation (blue), as compared to the smooth CAK start model (red, dashed), see text. **Middle:** Observed IUE spectra of the C IV $\lambda\lambda$1548, 1551 resonance doublet in ζ Pup, as function of line-of-sight velocity of the blue component. Overlayed are profiles calculated from CAK and LDI models, where the latter synthetic spectrum is computed using an extension of the technique developed in Sundqvist et al. (2010, 2011b), which takes 1-D snapshots and phase them randomly in patches of a parametrized angular size, here of 1°. **Right:** Density contours from a 2-D LDI simulation, in which the $\Delta\phi = 12$° wedges represent a clockwise time sequence starting from the initial CAK model. Adapted from Dessart & Owocki (2003).

The presence of strong, embedded wind shocks in LDI simulations provides a generally accepted explanation for the X-rays observed from single hot, massive stars without very strong magnetic fields, as further discussed by, e.g., Owocki et al. (2011) in this volume. In simulations with self-excited structure though, there is not enough material going through strong enough shocks to produce the observed amount of X-rays. But as shown by Feldmeier et al. (1997), introducing base perturbations such as those considered here enhances the velocity dispersion of the wind clumps, whereby clump-clump collisions create regions of relatively dense, hot gas. This then increases the X-ray emission to levels more comparable to those typically observed.

Because of the computational expense of calculating the line-force at each time step, LDI simulations have generally been limited to 1-D. More realistically though, thin shell instabilities and associated effects can be expected to break up the spherical shell structure into a more complex multi-dimensional structure. First attempts to con-

struct 2-D LDI simulations have been carried out by Dessart & Owocki (2003, 2005a). Such models typically show that the LDI first manifests itself as strong density compressions mimicking corresponding 1-D simulations. But as these initial shell structures are accelerated outwards, they become disrupted by Rayleigh-Taylor and thin-shell instabilities, which in the simulations by Dessart & Owocki (2003) operate all the way down to the azimuthal grid scale (Fig. 2, right panel). Moreover, these 2-D simulations have higher velocity dispersion than corresponding 1-D ones. Similarly as for the models with base perturbations just discussed then, this suggests an increase also in the amount of X-rays produced.

However, it may well be that these initial 2-D models exaggerate somewhat the level of lateral disruption, as they do not yet properly treat the lateral component of the diffuse line drag. Presuming this could damp azimuthal velocity perturbations on scales below the lateral Sobolev length $L_\phi = rv_{th}/v_r$ (Rybicki et al. 1990), lateral breakup may be prohibited below scales of order $\Delta\phi \approx L_\phi/r \approx v_{th}/v_r \approx 0.5°$. Future work should examine this issue by an adequate incorporation of the lateral line-force into multi-D LDI simulations.

3. Observations

3.1. Line profile variability

The most direct evidence for clumping in hot star winds comes from observations of narrow, spectral subpeaks superimposed on broad optical emission lines in Wolf-Rayet (WR) stars (Moffat et al. 1988; Robert 1994). Careful time-monitoring have revealed how these subpeaks, which trace local wind density enhancements, systematically migrate from line center toward line edges on time scales that can be associated with the wind acceleration. Indeed, Dessart & Owocki (2005b) showed that synthetic spectra calculated directly from LDI models can match well the observed migration in WR winds; however, the inferred acceleration scale typically predicts either a more extended acceleration zone than dynamically expected for line driven winds, or a much larger core radii than expected for WR stars (see also Lépine & Moffat 1999).

While predominately observed in dense WR winds, Eversberg et al. (1998) and Lépine & Moffat (2008) have provided first evidence of emission substructures also in O-stars, suggesting the phenomenon is universal in hot star winds. Moreover, Eversberg et al. (1998) pointed out that the density enhancements in ζ Pup always seemed to appear very near the stellar surface, thus providing an early indication of clumping close to the wind base (see Sect. 5). Further monitoring of such emission lines formed mainly in the inner wind would provide crucial information regarding clumping and wind acceleration in this key region.

3.2. The absorption troughs of saturated P Cygni lines

Instability simulations predict extensive structure not only in density, but also in velocity (Fig. 1, left panel). The most clear-cut evidence for such velocity structure in hot star winds comes from the extended regions of zero residual flux observed in saturated UV resonance lines (Fig. 1, middle panel). Already Lucy (1982) suggested that the physical origin of these 'black troughs' is the non-monotonic wind velocity field, which leads to enhanced back-scattering in multiple resonance zones and thereby to a systematic reduction of the blue-shifted emission. The middle panel of Fig. 1 demonstrates that

the velocity structure predicted by LDI simulations well reproduces the observed characteristics, whereas the monotonic velocity law of the CAK comparison model fails to reproduce in particular the blue edge of the line profile. This clearly indicates the presence of material with velocities well above the wind terminal speed v_∞ that sets the maximum blue-shifted absorption in a CAK model.[1]

4.   Diagnostics: deriving mass-loss rates from clumped hot star winds

Due to the rather steady wind base, the average mass-flux in the simulations described in Sect. 2 is actually not much affected by the LDI, which may indicate only second order effects on theoretical mass-loss rates predicted by steady-state models. But let us now discuss, arguably, *the* key question concerning wind clumping, namely how the structures in density and velocity affect the various diagnostics used to infer mass-loss rates from *observations*.

4.1.   Optically thin clumping

Traditionally most diagnostic studies aiming to derive mass-loss rates have assumed that the wind consists of statistically distributed *optically thin* clumps embedded in a void background medium, and neglected any disturbances on the velocity field. The main effect of such optically thin clumping is that diagnostics having opacities that scale with the local density squared, such as H_α and thermal IR/radio free-free emission, are stronger than in a smooth wind with the same mass-loss rate. The scaling invariant is $\sqrt{f_{cl}}\dot{M}$, i.e. mass-loss rates derived from H_α and smooth wind models are overestimated with the square-root of the clumping factor $f_{cl} \equiv \langle\rho^2\rangle/\langle\rho\rangle^2$ in the H_α line forming region. In contrast, diagnostics having opacities that scale linearly with density, such as UV resonance lines, electron scattering wings, and bound-free absorption of X-rays, are not directly affected by optically thin clumping[2].

For WR-stars, optically thin clumping has been accounted for since the pioneering work by Hillier (1991). Simultaneous fitting of electron scattering wings (scaling linearly with density) and emission peaks (density-squared) of optical recombination lines indicate $f_{cl} \sim 4$-20, corresponding to mass-loss reductions by factors of ~ 2-4 (see review by Crowther 2007). For O stars, electron scattering wings are too weak for this technique to be of use. But combined H_α/IR/radio studies (Puls et al. 2006) yield upper limit mass-loss rates that, similarly, are factors of ~ 2-4 lower than earlier H_α rates based on smooth wind models, and recent X-ray line attenuation studies confirm such reductions also on an absolute scale (Cohen et al. 2010, 2011). However, unsaturated UV resonance lines often suggest much more drastic reductions (Bouret et al. 2003, 2005; Prinja et al. 2005). The most prominent example in this respect has been the analysis of phosphorus v (Pv) in 40 Galactic O stars by Fullerton et al. (2006), who derived values of the mean ionization fraction times the mass-loss rate, $\langle q_{pv}\rangle\dot{M}$, that were factors of $10\ldots100$ lower than corresponding $\dot{M}$ values derived from smooth models

---

[1]The only way these features can be modeled within the context of a smooth outflow is by introducing a highly supersonic 'micro-turbulence' (Hamann 1981), typically on the order of ~ 5-10 % of the terminal speed.

[2]They can be indirectly affected though, through a modified wind ionization balance due to increased recombination rates, e.g. Bouret et al. (2003).

and H_α/radio emission. Since state-of-the-art non-LTE model atmospheres that include optically thin clumping typically predict $\langle q_{pv} \rangle \approx 1$ for early to mid type O stars, these Pv results seem to imply extremely low mass-loss rates, thus challenging the validity of the line-driven wind theory.

4.2. Optically thick clumping: porosity and vorosity

It is important to realize that the above results all rely on the assertion that individual clumps are optically thin; if this is not true for the investigated process, additional effects become important in the radiation transfer. Namely, optically thick clumps lead to a local self-shielding of opacity within the clumps, which in turn allows for increased escape of radiation through porous channels in between the clumps. The essential effect of such *porosity* is to reduce the medium's effective opacity as compared to an optically thin clump model (Feldmeier et al. 2003; Owocki et al. 2004); Fig. 2 graphically illustrates this general increase in transparency for porous media. The trade-off between porosity and mass-loss rate thus opposes the trade-off for density-squared diagnostics between optically thin clumping and mass-loss rate , i.e. neglecting porosity in cases where it is important can lead to *underestimated* mass-loss rates.
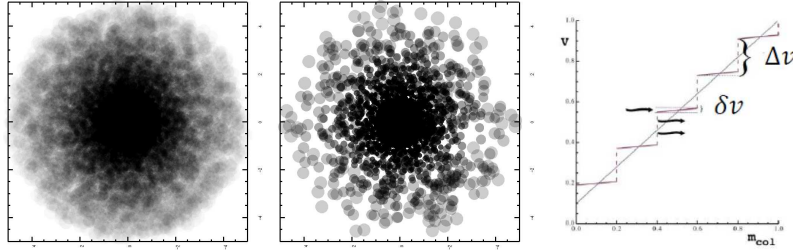
Figure 2.   **Left, middle:** Randomly generated isotropic clumps of length scales $\ell_{cl} \sim 0.1r$ and velocity-stretch porosity with $h_\infty = 0.5R_*$ (left) and $h_\infty = 5.0R_*$ (middle), that are lit from behind by a uniform source. Adapted from Sundqvist et al. (2011a). **Right:** Phenomenological velocity stair-case model vs. wind mass, where the dense clumps have velocity spans δv that are separated by an amount Δv. Here the associated velocity filling factor is $f_{vel} = \delta v/\Delta v = 1/10$ and the straight line represents a smooth CAK velocity law. Adapted from Owocki (2008).

Porosity in continuum absorption of X-rays? For *continuum* processes, the key parameter controlling to which extent porosity might be important is the so-called porosity length, defined as the mean free path between clumps and also equal to the clump length scale times the clumping factor, $h = \ell_{cl} f_{cl}$. Simplified porosity wind models have been applied to bound-free X-ray attenuation in O-star winds (Feldmeier et al. 2003; Oskinova et al. 2004, 2006; Owocki & Cohen 2006). The specific results of these studies depend on whether isotropic or anisotropic clumps are assumed, where the latter tends to enhance porosity effects (Oskinova et al. 2006; Sundqvist et al. 2011a). A key result for isotropic porosity is that it is quite difficult to make individual clumps optically thick, simply because the total integrated optical depths are quite low for X-ray absorption in O stars (Cohen et al. 2010, 2011). For 'velocity stretch' models in which the porosity length scales with the local wind velocity, $h = h_\infty(v/v_\infty)$, terminal porosity lengths well above a stellar radius typically are required for a significant effect (Cohen et al. 2008; Sundqvist et al. 2011a). Therefore it seems rather unlikely that porosity from LDI structure could have a significant effect on X-ray line profiles; even

though velocity stretching and clump-clump collisions in 1-D LDI models can cause clump separations in the outer wind to become on the order of a stellar radius, clump separations at lower radii tend to be much smaller, on the order of the Sobolev length $L_{\text{sob}} = v_{\text{th}}/(dv/dr) \approx (v_{\text{th}}/v)R_* \approx 0.01R_*$. The left panel of Fig. 3 demonstrates explicitly that X-ray line profiles with an opacity computed directly from the LDI density structures described in Sect. 2 are very similar to profiles computed using a smooth CAK model, indicating small porosity effects.

Vorosity in resonance line absorption? Contrasted to the case of continuum absorption discussed thus far, clumps can easily become optically thick in the inherently very strong UV resonance lines, as first pointed out by Oskinova et al. (2007). In a rapidly accelerating stellar wind, each *line* photon can only interact with the wind material within a very narrow spatial range, due to the narrow Doppler width of the line profile. This makes it possible for line photons to leak through the wind via 'porous' channels in velocity space, without ever interacting with the optically thick clumps (Fig. 2, right-most panel); hence this effect has been dubbed velocity porosity, or 'vorosity' (Owocki 2008). For a simple model with zero thermal speed, such vorosity may be characterized using solely a *velocity* filling factor $f_{\text{vel}} \equiv \delta v/\Delta v$, as defined in Fig. 2. The basic point though, is that this photon leakage in velocity space produces the same general effect as spatial porosity, namely a reduction in effective opacity as compared to an optically thin clump model.

Prinja & Massa (2010) found empirical evidence for such optically thick clumping by analyzing the Si IV resonance doublet in B supergiants. As these resonance lines are unaffected by optically thin clumps, the optical depth ratio between the blue and red line components should reflect the underlying atomic physics, i.e. $\tau_{\text{b}}/\tau_{\text{r}} = f_{\text{b}}/f_{\text{r}} = 2.0$ where f is the oscillator strength, *if* clumps were indeed optically thin. However, the ratios inferred by Prinja & Massa (2010) spread over the range ~ 1 to 2, with a mean $\tau_{\text{b}}/\tau_{\text{r}} = 1.5 \pm 0.3$ derived from their core sample of 25 stars. This result is a clear signature of optically thick clumps, and $\tau_{\text{b}}/\tau_{\text{r}} \approx 1.5$ has been shown to be consistent with calculations using the analytic vorosity models by Sundqvist et al. (2011b).

The fact that clumps seem to be optically thick in UV resonance lines may then also help explain the unexpected weakness of observed UV lines such as Pv (Sect. 4.1), as demonstrated by first attempts to include corresponding effects in line diagnostics (Oskinova et al. 2007; Hillier 2008; Sundqvist et al. 2010, 2011b; Šurlan 2011). Sundqvist et al. (2011b) analyzed Pv and H_α in the Galactic O6 supergiant λ Cep, accounting for structures in density as well as for a non-monotonic velocity field. As H_α is rather unaffected by optically thick clumping in this O star, whereas the strengths of the Pv lines are substantially reduced (see also Oskinova et al. 2007, for similar results for ζ Pup), the derived mass-loss rate is now only a factor of two lower than the prediction by Vink et al. (2000). This significantly alleviates previous discrepancies, and suggests that only mild reductions of current theoretical mass-loss rates are necessary.

However, while the middle panel of Fig. 3 demonstrates that vorosity is indeed present also in LDI simulations, the resulting absorption reduction is generally less than needed to fully explain the Pv observations (see also Owocki 2008). This may indicate that the present generation of LDI simulations do not properly resolve the internal clump velocity structures, and thus overpredict the clump velocity spans δv. Moreover, another problem with these simulations is that they do not show enough structure in the inner wind to reproduce the observed H_α emission (Sundqvist et al. 2011b). We

conclude this review by briefly discussing this discrepancy between predicted structure and observationally inferred clumping factors in the inner wind.
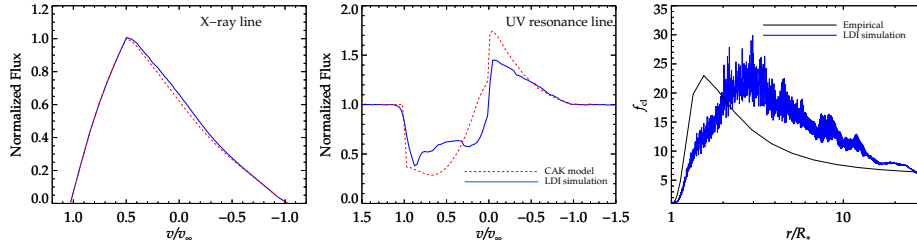

Figure 3. **Left, middle:** X-ray (left) and UV resonance (middle) line profiles for optical depths typical for ζ Pup at ~ 15 Å and for the Pv doublet. Adapted from Sundqvist et al. (2011a,b). **Right:** Radial stratification of the clumping factor as derived for ζ Pup by Najarro et al. (2011) (black) vs. theoretical predictions averaged over ~ 1000 1-D LDI snapshots (blue). The same 1-D LDI simulations and synthesis calculation methods as in Fig. 1 are used.

5. Clumping in the inner wind

The right panel of Fig. 3 compares predictions from LDI simulations with the radial stratification of $f_{\rm cl}$ for ζ Pup, as recently derived from the comprehensive multi-diagnostic study by Najarro et al. (2011). While the agreement is good both in terms of general behavior and in terms of absolute amount of clumping in the outer wind, the observationally inferred clumping law peaks at much lower radii than the theoretical one.

Considering the multitude of independent observational studies indicating similar results (Eversberg et al. 1998; Bouret et al. 2003; Puls et al. 2006; Cohen et al. 2011), this motivates a re-investigation of the onset of wind structure predicted by standard LDI simulations. Note that while the LDI simulation displayed here does include base perturbations, it still relies on the SSF formalism for calculating the line force and the associated diffuse line drag (Sect. 2). This probably overestimates the damping of perturbations close to the wind base, as suggested by first attempts to incorporate a more sophisticated escape integral source function (EISF) into LDI models (Owocki & Puls 1999). Along with suitable base perturbations, future work will implement various forms of such EISFs into a new generation of LDI simulations, and examine to what extent this may induce substantial structure also near the wind base.

References

Bouret, J.-C., Lanz, T., & Hillier, D. J. 2005, A&A, 438, 301
Bouret, J.-C., Lanz, T., Hillier, D. J., Heap, S. R., Hubeny, I., Lennon, D. J., Smith, L. J., & Evans, C. J. 2003, ApJ, 595, 1182
Carlberg, R. G. 1980, ApJ, 241, 1131
Castor, J. I., Abbott, D. C., & Klein, R. I. 1975, ApJ, 195

Cohen, D. H., Gagné, M., Leutenegger, M. A., MacArthur, J. P., Wollman, E. E., Sundqvist, J. O., Fullerton, A. W., & Owocki, S. P. 2011, MNRAS, 415, 3354

Cohen, D. H., Leutenegger, M. A., & Townsend, R. H. D. 2008, in Clumping in Hot-Star Winds, edited by W.-R. Hamann, A. Feldmeier, & L. M. Oskinova, 209

Cohen, D. H., Leutenegger, M. A., Wollman, E. E., Zsargó, J., Hillier, D. J., Townsend, R. H. D., & Owocki, S. P. 2010, MNRAS, 405, 2391

Crowther, P. A. 2007, ARA&A, 45, 177

Dessart, L., & Owocki, S. P. 2003, A&A, 406, L1

— 2005a, A&A, 437, 657

— 2005b, A&A, 432, 281

Eversberg, T., Lepine, S., & Moffat, A. F. J. 1998, ApJ, 494, 799

Feldmeier, A. 1995, A&A, 299, 523

Feldmeier, A., Oskinova, L., & Hamann, W.-R. 2003, A&A, 403, 217

Feldmeier, A., Puls, J., & Pauldrach, A. W. A. 1997, A&A, 322, 878

Fullerton, A. W., Massa, D. L., & Prinja, R. K. 2006, ApJ, 637, 1025

Hamann, W.-R. 1981, A&A, 93, 353

Hamann, W.-R., Feldmeier, A., & Oskinova, L. M. (eds.) 2008, Clumping in hot-star winds

Hillier, D. J. 1991, A&A, 247, 455

— 2008, in Clumping in Hot-Star Winds, edited by W.-R. Hamann, A. Feldmeier, & L. M. Oskinova, 93

Lépine, S., & Moffat, A. F. J. 1999, ApJ, 514, 909

— 2008, AJ, 136, 548

Lucy, L. B. 1984, ApJ, 284, 351

MacGregor, K. B., Hartmann, L., & Raymond, J. C. 1979, ApJ, 231, 514

Moffat, A. F. J., Drissen, L., Lamontagne, R., & Robert, C. 1988, ApJ, 334, 1038

Najarro, F., Hanson, M. M., & Puls, J. 2011, ArXiv e-prints. 1108.5752

Oskinova, L. M., Feldmeier, A., & Hamann, W.-R. 2004, A&A, 422, 675

— 2006, MNRAS, 372, 313

Oskinova, L. M., Hamann, W.-R., & Feldmeier, A. 2007, A&A, 476, 1331

Owocki, S. P. 2008, in Clumping in Hot-Star Winds, edited by W.-R. Hamann, A. Feldmeier, & L. M. Oskinova, 121

Owocki, S. P., Castor, J. I., & Rybicki, G. B. 1988, ApJ, 335, 914

Owocki, S. P., & Cohen, D. H. 2006, ApJ, 648, 565

Owocki, S. P., Gayley, K. G., & Shaviv, N. J. 2004, ApJ, 616, 525

Owocki, S. P., & Puls, J. 1996, ApJ, 462, 894

— 1999, ApJ, 510, 355

Owocki, S. P., & Rybicki, G. B. 1984, ApJ, 284, 337

Owocki, S. P., Sundqvist, J. O., Cohen, D. H. D., & Gayley, K. G. 2011, in Four decades of Research on Massive Stars, edited by C. Robert, N. St-Louis, & L. Drissen

Prinja, R. K., Massa, D., & Searle, S. C. 2005, A&A, 430, L41

Prinja, R. K., & Massa, D. L. 2010, A&A, 521, L55+

Puls, J., Markova, N., Scuderi, S., Stanghellini, C., Taranova, O. G., Burnley, A. W., & Howarth, I. D. 2006, A&A, 454, 625

Puls, J., Vink, J. S., & Najarro, F. 2008, A&A Rev., 16, 209

Robert, C. 1994, Ap&SS, 221, 137

Runacres, M. C., & Owocki, S. P. 2002, A&A, 381, 1015

— 2005, A&A, 429, 323

Rybicki, G. B., Owocki, S. P., & Castor, J. I. 1990, ApJ, 349, 274

Sundqvist, J. O., Owocki, S., Cohen, D., Leutenegger, M. A., & Townsend, R. 2011a, MNRAS, submitted

Sundqvist, J. O., Puls, J., & Feldmeier, A. 2010, A&A, 510, A11

Sundqvist, J. O., Puls, J., Feldmeier, A., & Owocki, S. P. 2011b, A&A, 528, A64

Šurlan, B. 2011, in Four decades of Research on Massive Stars, edited by C. Robert, N. St-Louis, & L. Drissen

Vink, J. S., de Koter, A., & Lamers, H. J. G. L. M. 2000, A&A, 362, 295